

Red Light Modulates Ultraviolet-Induced Gene Expression in the Epidermis of Hairless Mice

Max Myakishev-Rempel, PhD,¹ Istvan Stadler, PhD,² Oksana Polesskaya, PhD,³ Alifiya S. Motiwala, PhD,⁴ Frances Barg Nardia, MS,¹ Benjamin Mintz, PhD,³ Ancha Baranova, PhD,^{4,5,6} James Zavislan, PhD,³ and Raymond J. Lanzafame, MD, MBA⁷

Abstract

Objective: The purpose of this study was to investigate whether low-level light therapy (LLLT) was capable of modulating expression of ultraviolet (UV) light-responsive genes *in vivo*. **Materials and methods:** The effects of 670 nm light-emitting diode (LED) array irradiation were investigated in a hairless SHK-1 mouse epidermis model. Mice were given a single dose of UVA/UVB light, or three doses of red light (670 nm @ 8 mW/cm² x 312 sec, 2.5 J/cm² per session) spread over 24 h along with combinations of pre- and post-UV treatment with red light. Levels of 14 UV-responsive mRNAs were quantified 24 h after UV irradiation by real-time quantitative reverse transcription polymerase chain reaction (qRT-PCR). **Results:** The transcription of mRNAs encoding for cluster of differentiation molecule 11b (CD11b) ($p < 0.05$) and interferon (IFN)- γ ($p < 0.012$) increased after irradiation with red light alone, whereas expression level of cyclooxygenase (COX)-2 ($p < 0.02$) was down-regulated. Genes unresponsive to UV did not change their expression levels after exposure to red light either. Pretreatment with red light significantly modified response of Fos to UV exposure ($p < 0.01$). A synergy of UV and post-treatment with red light in reducing the transcription levels of CD11b ($p < 0.05$) and inducible nitric oxide synthase (iNOS) ($p < 0.05$) was observed. **Conclusions:** This is an initial observation that in mouse red light LLLT more often than not causes opposite gene expression changes or reduces those caused by moderate UVA-UVB irradiation.

Introduction

LOW-LEVEL LIGHT THERAPY (LLLT) or photobiomodulation (PBM) frequently employs red and near infrared (NIR) light (600–1000 nm) for treating skin disorders. Since its introduction in 1967, it has been adopted for reducing pain and inflammation, augmenting tissue repair, and promoting regeneration of damaged tissues.¹ Even at the low doses used in LLLT, irradiation with red light results in complex changes in the gene expression program.^{2,3} The most likely mechanism of the therapeutic action of LLLT is the alleviation of mitochondrial dysfunction through the reduction of oxidative stress, which, in turn, improves cell metabolism and reduces inflammation.^{3,4}

On the other hand, the predominantly damaging effects of ultraviolet (UV) irradiation are well studied. UV induces

DNA damage and activates the associated repair mechanisms in many cell and animal models, including direct UV irradiation of the skin.^{5,6} Several recent studies (reviewed in the article by Barolet and Boucher⁷) suggest that red and NIR light exposure may protect against UV-induced skin damage. In particular, repetitive irradiation of humans with 660 nm red light reduces their consequent response to UV light in a way similar to sun protection factor-15 (SPF15) sunscreen.⁷ However, the underlying molecular mechanisms of the effect of red light LLLT on the tissue response to short-term UV exposure are largely unknown.

To date, a majority of studies concerning the effects of red light on gene expression patterns have been performed using cultured fibroblasts,^{2,8–12} with only a few studies completed in animals.^{13–15} Here, we describe the effects of red light exposure on expression patterns of select genes in the

¹Localized Therapeutics LLC, Chicago, Illinois.

²Rochester General Hospital, Rochester, New York.

³University of Rochester, Microbiology and Immunology, Rochester, New York.

⁴School of Systems Biology, George Mason University, Manassas, Virginia.

⁵Research Center for Medical Genetics, Moscow, Russian Federation.

⁶Moscow Institute of Physics and Technology (State University), Institutskii Pereulok, Moscow Region, Russia.

⁷MD PLLC, Rochester, New York.

epidermis, in a well-established hairless SKH-1 mouse model.^{16,17} In particular, we profiled an expression of genes involved in wound remodeling and healing,^{18,19} and studied whether the exposure to red LLLT produced by light-emitting diode (LED) array was capable of attenuating the effects of UV light on gene expression in the live healthy epidermis.

Materials and Methods

Animals

The experiment was conducted in the Laboratory of Laser Surgery of Rochester General Hospital using 4- to 6-week-old female SKH-1 mice (Charles River Laboratories, Wilmington, MA). SKH-1 strain mice are albino background mice with fully functional immunity and health except for a dysfunctional hair cycle gene *Hr1* resulting in near absence of hair, which makes them a preferred model for photo-irradiation studies.^{20,21} All procedures were approved by the Institutional Animal Care Committee. All irradiations were administered on days 5–7 after arrival.

UV treatment

The home cages were covered with custom lids made by covering the top with 1 mm chicken wire net at 9 mm pitch. UV light source as described²¹ was composed of a bank of four UV lamps (Q-Lab, Cat. UVA-340) installed in a generic 4-fluorescent-lamp fixture (Utilitech, Cat. 184346). UVA-340 lamps emit light between 295 and 390 nm, covering both UVA and UVB parts of the spectrum. The inner surface of the fixture was covered with aluminum foil for better reflection. The fluence was measured using IL1700 light meter (International Light Technologies, Peabody, MA) and an SED240 UVB probe and an SED005 UVA probe to provide $23 \mu\text{W}/\text{cm}^2$ UVB and $1.4 \text{ mW}/\text{cm}^2$ UVA at the level of the mice's backs. The mice were irradiated from above at a distance of 35 cm from the lamps to the mice. The UV

treatment consisted of a single irradiation for 2 h 23 min, which corresponds to a cumulative dose of $200 \text{ mJ}/\text{cm}^2$ UVB and $11.8 \text{ J}/\text{cm}^2$ UVA at the level of the mice (Fig. 1.). This regimen was selected based on previous studies^{21,22} to result in a moderate UV burn, which would become visible by the end of treatment, peak in 1.5 days, and heal by days 7–9.

Red light treatment

The red light source was custom built by Kodak (Eastman Kodak, Rochester, NY) to fit, power, and cool three LED arrays developed by Quantum Devices (Barneveld, WI) for NASA research.²³ Each LED array was composed of 91 hybrid gallium-aluminum-arsenide (GaAlAs) LEDs. The outputs were measured and mapped over their entire surface using a Newport 835-C Power meter equipped with an 818 SL detector head (Newport Corp., Irvine, CA). An overall 85% light uniformity was achieved at the bottom of the cage. The source produced continuous noncoherent red light with a wide Gaussian-shaped spectral peak having a maximum at 670 nm and a median range of 655–685 nm ($670 \pm 20 \text{ nm}$). Whole-body irradiation was achieved by placing three awake, unanesthetized mice in a Plexiglas chamber with ventilated walls as described.²³ The mice were given three irradiations at $8 \text{ mW}/\text{cm}^2$ fluence for 312 sec each during a period of 24 h, resulting in a total dose density of $2.5 \text{ J}/\text{cm}^2$ per session ($7.5 \text{ J}/\text{cm}^2$ for three sessions) (Fig. 1).

Treatment groups

The treatment groups and treatments are summarized in Fig. 1. The time dependence of red light exposure was tested in two scenarios. UV irradiation was started 1 h after the last red light treatment in Group 4 to provide the time for gene expression changes, and red light treatment was started

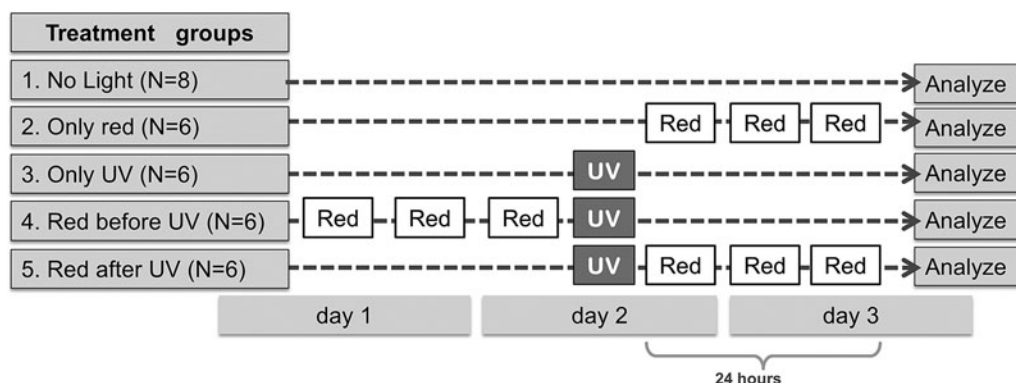


FIG. 1. Treatment groups and treatments. The mice from an immune-competent hairless SKH-1 strain were divided into five groups and treated in parallel. Both types of light were administered as whole body irradiation. Red light irradiation was produced with $670 \pm 20 \text{ nm}$ light-emitting diode (LED) array and consisted of three sessions lasting 5 min 12 sec each, delivered over a period of 24 h, delivering a fluence of $8 \text{ mW}/\text{cm}^2$ and resulting in a cumulative dose density of $2.5 \text{ J}/\text{cm}^2$ per session ($7.5 \text{ J}/\text{cm}^2$ for three sessions). Ultraviolet (UV) light irradiation was produced with a 295–390 nm bank of UVA-UVB tube lights and consisted of one session at $23 \mu\text{W}/\text{cm}^2$ UVB and $1.4 \text{ mW}/\text{cm}^2$ UVA fluence lasting 2 h 23 min resulted in a cumulative dose density of $200 \text{ mJ}/\text{cm}^2$ UVB and $11.8 \text{ J}/\text{cm}^2$ UVA. The mice were euthanized 1 h after the last irradiation and select epidermal mRNAs were quantified.

immediately after the end of UV irradiation in Group 5 because UV irradiation was sufficiently long (2.4 h) for the gene expression changes to take place.

Sample preparation

The mice were euthanized by CO₂ in their home cages. Next, the backs were flattened by soft palpation to facilitate later scraping. The mice were briefly wrapped in paper towels, and placed individually under crushed dry ice. Upon complete freezing, the mice were stored in a -70°C freezer. Later, areas of epidermis from skin that had been facing the UV lamps were scraped from the back of each frozen mouse in a cold CO₂ atmosphere (~-10°C, over crushed dry ice in a large styrofoam box) into a cold plastic Petri dish using a disposable scalpel. The scraping uniformly covered an area of 9 cm² and was stopped when the amount of scraped material reached 60–80 mg. The epidermal powder was placed in 1.3 mL room temperature Trizol (Sigma, St. Louis, MO) using a pipette with a truncated 1 mL tip, then frozen on dry ice and stored at -20°C.

RNA extraction

Samples were thawed in room temperature water bath. Zirconia beads (1 mm diameter, Biospec Products, Bartlesville, OK) were added to fill the tube completely, and the sample was homogenized by shaking in Mini-Beadbeater (Biospec Products) for 3 min. The homogenate was transferred into a new tube, centrifuged at 12,000g for 15 min at 4°C. The aqueous phase was transferred into a new tube, frozen and stored at -20°C. The samples were thawed at room temperature, chloroform was added to final 20% v/v, and samples were vortexed, incubated for 3 min, vortexed again, and centrifuged for 15 min at 4°C. The clear top fraction of the supernatant was mixed with an equal volume of 70% ethanol, and loaded onto Purelink columns (Micro-to-Midi kit, Invitrogen, Waltham, MA). DNase cocktail was loaded on the column and RNA was extracted according to the manufacturer's protocol beginning with the addition of Wash Buffer I. Yield and quality of RNA were determined by 260/280 nm absorption spectrum using Nanodrop (Nanodrop, Wilmington, DE).

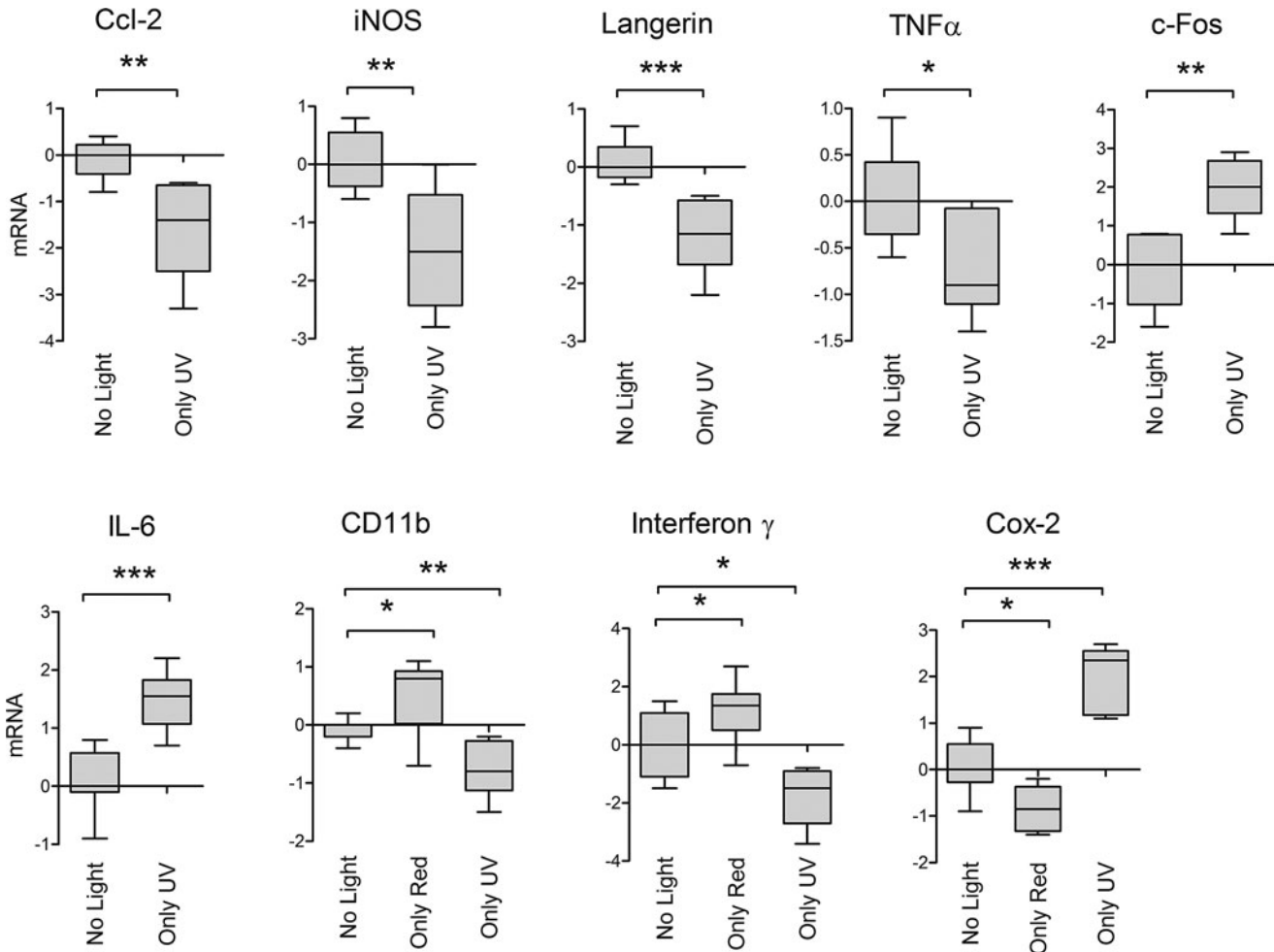


FIG. 2. Selected epidermal transcripts were quantified by TaqMan assays. The number of mice per group (6 or 8) is shown in Fig. 1. Each transcript was normalized to an average of β -actin and glyceraldehyde 3-phosphate dehydrogenase (GAPDH). Cycle threshold (Ct) values of each sample were averaged per treatment group and normalized to the “no light” group, resulting in normalized log-copy number averages, which were plotted. Boxes indicate 1st and 3rd quartiles, whiskers indicate min and max values. (* $p \leq 0.05$, ** $p \leq 0.01$, *** $p \leq 0.001$ by Mann–Whitney rank sum test.)

Real-time reverse transcription polymerase chain reaction (RT PCR)

cDNA was synthesized using a Superscript III first-strand synthesis kit with random hexamer primer (Life Technologies, Grand Island, NY) and quantified by TaqMan RT PCR using TaqMan assays (Life Technologies, Grand Island, NY) for 13 genes: interleukin-6 (IL-6), cyclooxygenase (COX)-2, c-Fos, inducible nitric oxide synthase (iNOS), c-Jun, Langerin (CD207), chemokine (C-C motif) ligand 2 (Ccl-2), IL-4, interferon- γ (IFN- γ), tumor necrosis factor α (TNF- α), cluster of differentiation molecule 11b (CD11b), B cell surface antigen CD40, and cytosolic phospholipase A2 (cPlA2).

The concentration of mRNA was normalized by a log average of two housekeeping genes, β -actin and glyceraldehyde 3-phosphate dehydrogenase (GAPDH). The fact that cycle thresholds (Ct) for β -actin and GAPDH were in good agreement suggested that neither of them was affected by UV and red light treatments, and, therefore, that they could be used as reference genes. All TaqMan assays were performed with manufacturer-specified parameters in 96-well plates using iCycler (BioRad, Hercules, CA). Melting curves were used to validate product specificity. All samples were amplified in triplicate from the same total RNA preparation, and the mean value was used for further analysis. Ct values of target genes >37 were considered to be a negative call, and assigned a value = 37 for the purpose of normalization. Ct values of control wells (i.e., no-template control, positive control) were examined for each plate. *p*-Values for pairwise comparison of treatment groups were calculated by Mann-Whitney rank sum test assuming equal variance and quasinormal distribution of Cts. The graphs normalized to no light treatment and plotted in GraphPad Prizm (GraphPad Software, La Jolla, CA).

Results

Selection of UV-responsive genes

We selected 13 genes for this study, namely, (IL-6), COX-2, [also prostaglandin-endoperoxide synthase 2 (P_{ts}g2)], c-Fos (Fos), iNOS (also Nos2), c-Jun (Jun), Langerin (CD207), Ccl-2, IL-4, IFN- γ (also Ifng), TNF- α , cCD11b, ITGAM, B cell surface antigen CD40, and cPlA2, and Pla2g4a. All these genes were previously identified as UV inducible in a variety of experimental systems.^{18,19}

Four of these genes, Jun, cPlA2, CD40, and IL-4, did not significantly change their expression in the skin of UV-irradiated mice, and were excluded from further discussion.

After exposure to UV light, the expression levels significantly changed for 9 out of 13 genes. The transcription of mRNAs encoding for Ccl2 (*p*<0.006, all *p* values by Mann-Whitney rank sum test), CD11b (*p*<0.008), IFN- γ (*p*<0.03), iNOS (*p*<0.009), Langerin (*p*<0.0007), and TNF- α (*p*<0.045) were decreased after UV irradiation, whereas COX-2 (*p*<0.0007), c-Fos (*p*<0.006), and IL-6 (*p*<0.005) were upregulated (Fig. 2).

Effect of red light alone on expression of "UV-responsive" genes

Red light in the absence of UV caused a significant change for three out of the nine UV-responsive genes as

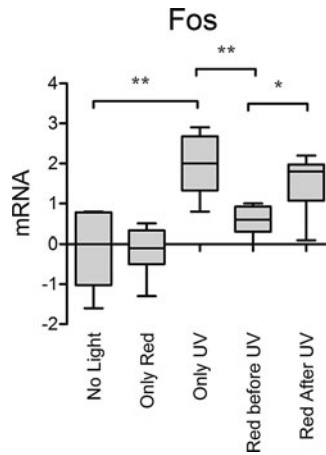


FIG. 3. Epidermal cFos transcript was quantified by TaqMan assay, cycle threshold (Ct) values were normalized to an average of β -actin and glyceraldehyde 3-phosphate dehydrogenase (GAPDH), averaged per treatment group, and each group was normalized to the "no light" group, resulting in normalized log-copy number averages, which were plotted. Boxes indicate 1st and 3rd quartiles, whiskers indicate min and max values. (**p*≤0.05, ***p*≤0.01, by Mann-Whitney rank sum test.)

compared with unirradiated skin. The mRNA levels of CD11b (*p*<0.05) and IFN- γ (*p*<0.012) increased after irradiation with red light alone, whereas the mRNA level of COX-2 (*p*<0.02) was downregulated (Fig. 2).

The expression levels of four genes that were not responding to UV irradiation in our experimental system – Jun, cPlA2, CD40, and IL-4 – were quantified both before and after exposure to red light, and were not significantly affected by red light either.

Pretreatment with red light modifies UV response of Fos

In skin samples of mice pretreated with red light before UV, the expression levels of Fos were significantly lower

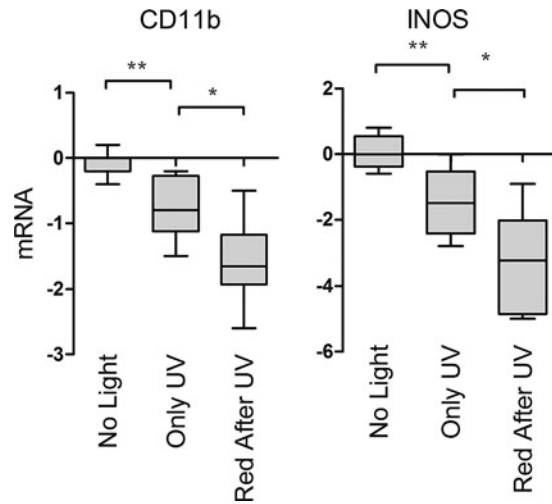


FIG. 4. Epidermal CD11b and inducible nitric oxide synthase (iNOS) transcripts were quantified by TaqMan assays, cycle threshold (Ct) values were normalized to an average of β -actin and glyceraldehyde 3-phosphate dehydrogenase (GAPDH), averaged per treatment group, and each group was normalized to the "no light" group, resulting in normalized log-copy number averages, which were plotted. Boxes indicate 1st and 3rd quartiles, whiskers indicate min and max values. (**p*≤0.05, ***p*≤0.01 by Mann-Whitney rank sum test.)

than those in mice treated with UV only ($p < 0.01$) (Fig. 3). There was no significant difference in the mRNA levels of Fos in untreated mice as compared with the mice receiving red light before UV.

Post-treatment with red light enhances UV response of iNOS and Cd11b

A synergy between UV and subsequent red light treatments was observed in the reduction of the mRNA levels of CD11b ($p < 0.05$) and iNOS ($p < 0.05$) (Fig. 4). The complete set of graphs is provided in Supplementary Fig. S1 (see supplementary material at www.liebertpub.com/pho).

Discussion

Because of its noninvasive nature and ease of use, LLLT is increasingly being used as an option to treat a multitude of conditions that require relief from or reduction of inflammation, and subsequent healing of the lesion. Several studies have suggested that LLLT may counter the acute inflammatory sequelae of cutaneous UV exposure. This makes the potential use of LLLT for skin damage prophylaxis and for the treatment of cutaneous sun burns an appealing possibility. However, the mechanisms for the beneficial effect of LLLT are poorly understood, in striking contrast to the substantial degree of understanding gleaned regarding the acute inflammatory and immunological events associated with cutaneous UV exposure.⁶ We subjected hairless SKH-1 mice to UV irradiation at a moderate dose accompanied by an exposure to red light in two modes, a preventive mode with red light pretreatment and a therapeutic mode with low-level red light exposure of UV-irradiated skin (Fig. 1) in order to obtain an insight into the mechanisms of LLLT protection in UV exposure-related skin damage. Expression levels for a number of genes known for their involvement in response to UV exposure were profiled at baseline and basic combinations of acute UV and red light, as is shown in Fig. 2.

Importantly, not every UV-responsive gene changes its expression in all experimental systems studied. In our *in vivo* model, 5 out of 14 UV-responsive genes, TNFRSF1A, Jun, *Pla2g4a*, CD40 and IL-4, did not significantly change their expression levels, and were excluded from further studies. Importantly, none of these genes changed their expression in response to red light exposure either.

Interestingly, three out of the nine UV-responsive genes were also responsive to red light alone. It is possible that the red light-dependent increase in expression of CD11b and IFN- γ can be explained by migration of CD11b+ infiltrating leukocytes into light-exposed skin. Irradiation with UV also increases infiltration with CD11b+ leukocytes that then would serve as a major source of oxidative stress in irradiated skin.²⁴ In keratinocytes, these reactive oxygen species (ROS) stimulate the NF- κ B pathway that, in turn, activates an expression of COX-2.^{25,26} Interestingly, in our model of LLLT, an increase in the levels of CD11b mRNA was accompanied by a decrease in expression levels of COX-2; therefore, ROS-producing CD11b+ leukocytes are unlikely to be a source of red light-induced increase in the expression of CD11b-encoding genes. Additional support of the hypothesis that red light induced an increase in the expression of CD11b-encoding mRNA may be that the response of

some other cellular type rests on the observation that the peak of UV-induced skin infiltration by leukocytes is observed between 48 and 72 h after UV exposure,²⁴ whereas we collected our samples <24 h after treatment with red light (Fig. 1). Recent studies showed that CD11b+ dermal dendritic cells have a phenotype that overlaps with that of dermal macrophages, and are substantially more abundant in steady state epidermis than in activated infiltrating cells.²⁷ It is tempting to speculate that an increase in expression of CD11b after LLLT was the result of *de novo* expression of the CD11b marker in the dendritic cells or other non-inflammatory skin dwellers.

Conclusions

The most important observation of our study was that pretreatment with red light substantially decreased the degree of UV stimulation in the expression of Fos, a component of the activator protein 1 (AP-1) transcription factor and a well-known regulator of cell proliferation, differentiation, and apoptosis.²⁸ In UV-irradiated skin, an induction of Fos results in an increase in the release of matrix metalloproteinases and subsequent erosion of the skin.^{29,30} Moreover, Fos is among the key molecular components contributing to DNA damage after exposure to UV light.³¹ Consistent with this observation, our results show a marked increase in Fos expression after exposure to UV, whereas pretreatment with the red light substantially alleviated an elevation in Fos-encoding mRNA. Post-treatment with LLLT also resulted in a trend toward a decrease in the magnitude of the Fos mRNA elevation, although the difference was not statistically significant. These observations indicate that therapeutic exposure to red light may decrease UV-mediated skin damage by modulating the Fos response.

Acknowledgments

This work was supported by the Kidd Fund, Rochester General Hospital Foundation, and was performed in Rochester General Hospital.

Author Disclosure Statement

No competing financial interests exist.

References

1. Avci P, Gupta A, Sadasivam M, et al. Low-level laser (light) therapy (LLLT) in skin: stimulating, healing, restoring. *Semin Cutan Med Surg* 2013 Mar; 32(1) 41–52.
2. Zhang Y, Song S, Fong C-C, Tsang C-H, Yang Z, Yang M. cDNA microarray analysis of gene expression profiles in human fibroblast cells irradiated with red light. *J Invest Dermatol* 2003;120:849–857.
3. Eells JT, Wong-Riley MT, VerHoeve J, et al. Mitochondrial signal transduction in accelerated wound and retinal healing by near-infrared light therapy. *Mitochondrion* 2004;4:559–567.
4. Tang J, Du Y, Lee CA, Talahalli R, Eells JT, Kern TS. Low-intensity far-red light inhibits early lesions that contribute to diabetic retinopathy: in vivo and in vitro. *Invest Ophthalmol Vis Sci* 2013;54:3681–3690.

5. Mancebo SE, Wang SQ. Skin cancer: role of ultraviolet radiation in carcinogenesis. *Rev Environ Health* 2014;29:265–273.
6. Clydesdale GJ, Dandie GW, Muller HK. Ultraviolet light induced injury: immunological and inflammatory effects. *Immunol Cell Biol* 2001;79:547–568.
7. Barolet D, Boucher A. LED photoprevention: reduced MED response following multiple LED exposures. *Lasers Surg Med* 2008;40:106–112.
8. Hawkins D, Abrahamse H. Effect of multiple exposures of low-level laser therapy on the cellular responses of wounded human skin fibroblasts. *Photomed Laser Surg* 2006;24:705–714.
9. AlGhamdi KM, Kumar A, Moussa NA. Low-level laser therapy: a useful technique for enhancing the proliferation of various cultured cells. *Lasers Med Sci* 2012;27:237–249.
10. Mirzaei M, Bayat M, Mosafa N, et al. Effect of low-level laser therapy on skin fibroblasts of streptozotocin-diabetic rats. *Photomed Laser Surg* 2007;25:519–525.
11. Peplow PV, Chung T-Y, Ryan B, Baxter GD. Laser photobiomodulation of gene expression and release of growth factors and cytokines from cells in culture: a review of human and animal studies. *Photomed Laser Surg* 2011;29:285–304.
12. Nomura K, Yamaguchi M, Abiko Y. Inhibition of interleukin-1 β production and gene expression in human gingival fibroblasts by low-energy laser irradiation. *Lasers Med Sci* 2001;16:218–223.
13. Safavi SM, Kazemi B, Esmaeili M, Fallah A, Modarresi A, Mir M. Effects of low-level He–Ne laser irradiation on the gene expression of IL-1 β , TNF- α , IFN- γ , TGF- β , bFGF, and PDGF in rat's gingiva. *Lasers Med Sci* 2008;23:331–335.
14. Rizzi CF, Mauriz JL, Freitas Corrêa DS, et al. Effects of low-level laser therapy (LLLT) on the nuclear factor (NF)- κ B signaling pathway in traumatized muscle. *Lasers Surg Med* 2006;38:704–713.
15. Aimbire F, Albertini R, Pacheco M, et al. Low-level laser therapy induces dose-dependent reduction of TNF α levels in acute inflammation. *Photomed Laser Surg* 2006;24:33–37.
16. Canfield PJ, Xu FN, Greenoak GE, Reeve VE, Gallagher CH, Wilkinson F. Ultrastructure of ultraviolet radiation-induced hairless mouse skin carcinogenesis, with special reference to the epidermal–dermal junction. *Pathology* 1986;18:337–344.
17. Cooper SJ, MacGowan J, Ranger–Moore J, Young MR, Colburn NH, Bowden GT. Expression of dominant negative c-jun inhibits ultraviolet B-induced squamous cell carcinoma number and size in an SKH-1 hairless mouse model. *National Institutes of Health Grants CA27502 and the Cancer Research Foundation of America Fellowship Grant. Mol Cancer Res* 2003;1:848–854.
18. Kremer IB, Cooper KD, Teunissen MB, Stevens SR. Low expression of CD40 and B7 on macrophages infiltrating UV-exposed human skin; role in IL-2/R α -T cell activation. *Eur J Immunol* 1998;28:2936–2946.
19. Stitzel ML, Durso R, Reese JC. The proteasome regulates the UV-induced activation of the AP-1-like transcription factor Gcn4. *Genes Dev* 2001;15:128–133.
20. Erdle BJ, Brouxhon S, Kaplan M, Vanbuskirk J, Pentland AP. Effects of continuous-wave (670-nm) red light on wound healing. *Dermatol Surg* 2008;34:320–325.
21. Myakishev–Rempel M, Stadler I, Brondon P, et al. A preliminary study of the safety of red light phototherapy of tissues harboring cancer. *Photomed Laser Surg* 2012;30:551–558.
22. Pentland AP, Scott G, VanBuskirk J, Tanck C, LaRossa G, Brouxhon S. Cyclooxygenase-1 deletion enhances apoptosis but does not protect against ultraviolet light-induced tumors. *Cancer Res* 2004;64:5587–5591.
23. Lanzafame RJ, Stadler I, Kurtz AF, et al. Reciprocity of exposure time and irradiance on energy density during photoradiation on wound healing in a murine pressure ulcer model. *Lasers Surg Med* 2007;39:534–542.
24. Mittal A, Elmets CA, Katiyar SK. CD11b+ cells are the major source of oxidative stress in UV radiation-irradiated skin: possible role in photoaging and photocarcinogenesis. *Photochem Photobiol* 2003;77:259–264.
25. Yang C, Ling H, Zhang M, et al. Oxidative stress mediates chemical hypoxia-induced injury and inflammation by activating NF-kappaB–COX-2 pathway in HaCaT cells. *Mol Cells* 2011;31:531–538.
26. Yang C, Yang Z, Zhang M, et al. Hydrogen sulfide protects against chemical hypoxia-induced cytotoxicity and inflammation in HaCaT cells through inhibition of ROS/NF- κ B/COX-2 pathway. *PLoS One* 2011;6:e21971.
27. Tamoutounour S, Guillemins M, Montanana Sanchis F, et al. Origins and functional specialization of macrophages and of conventional and monocyte-derived dendritic cells in mouse skin. *Immunity* 2013;39:925–938.
28. Vesely PW, Staber PB, Hoefler G, Kenner L. Translational regulation mechanisms of AP-1 proteins. *Mutation Res.* 2009;682:7–12.
29. Gack S, Vallon R, Schaper J, Ruther U, Angel P. Phenotypic alterations in fos-transgenic mice correlate with changes in Fos/Jun-dependent collagenase type I expression. Regulation of mouse metalloproteinases by carcinogens, tumor promoters, cAMP, and Fos oncoprotein. *J Biol Chem* 1994;269:10,363–10,369.
30. Hwang YP, Oh KN, Yun HJ, Jeong HG. The flavonoids apigenin and luteolin suppress ultraviolet A-induced matrix metalloproteinase-1 expression via MAPKs and AP-1-dependent signaling in HaCaT cells. *J Dermatol Sci* 2011;61:23–31.
31. Tornaletti S, Pfeifer GP. UV light as a footprinting agent: modulation of UV-induced DNA damage by transcription factors bound at the promoters of three human genes. *J Mol Biol* 1995;249:714–728.

Address correspondence to:
 Max Myakishev–Rempel
 2414 W. Byron St. Unit 2
 Chicago IL, 60618

E-mail: max@localizedtherapeutics.com